Support Information

A robust and thickness-insensitive hybrid cathode interlayer for high-efficiency and stable inverted organic solar cells

Ping Cai,*[a] Can Song,[a] Shiyun Lei,[b] Kanglin Yu,[b] Ling Ding,[a] Dianhui Wang,[a] Guiting Chen,[c] Hongliang Peng,[a] Bin Li,[a] Xunchang Wang,[b] Biao Xiao,*[b] Renqiang Yang*[b]

[a]*Guangxi Key Laboratory of Information Materials, School of Materials Science and Engineering, Guilin University of Electronic Technology, Guilin 541004, China. E-mail: caiping@guet.edu.cn*

[b]*Key Laboratory of Optoelectronic Chemical Materials and Devices (Ministry of Education), School of Optoelectronic Materials and Technology, Jianghan University, Wuhan 430056, China. E-mail: biaoxiao@jhun.edu.cn (B. Xiao) and yangrq@jhun.edu.cn (R. Yang)*

[c]*School of Chemistry and Environment, Jiaying University, Meizhou 514015, China.*

Experimental Section

Materials

PBDB-T, PM6, ITIC, Y6, L8-BO, BTP-eC9, and PDINN are purchased from Solarmer Energy Inc., and the chemical structures of active layer materials are shown in Fig. S1. The PFOPy polymer was synthesized based on the previously reported method [1]. Unless otherwise specified, all reagents were purchased from Merck or Acros Inc., and were directly used without further purification.

Device Fabrication

The device configuration of inverted OSCs is ITO/CIL/active layer/AIL/Ag. ITO glass substrate was successively cleaned in a sonication bath by detergent, deionized water, acetone, deionized water, and isopropyl alcohol for 15 min each at room temperature, and then dried for backup. The ZnO CIL was prepared by the sol-gel

method [1]. The PFOPy or PFOPy-N CILs was deposited on top of the UV/ozone-treated ITO substrate by spin-coating PFOPy or PFOPy-N solutions at 2000 rpm for 30 s and then thermally crosslinked at optimized temperature for 10 min, where the PFOPy-N blend solution was prepared by adding PDINN methanol solution into PFOPy methanol solution with different concentration and weight ratio of PDINN. PBDB-T:ITIC, PM6:Y6, PM6:L8-BO, and PM6:BTP-eC9 active layers were separately spin-coated on CIL by previously optimized methods [1, 2-4]. Finally, 10 nm MoO_3 AIL and 100 nm Ag anode were successively deposited by thermal evaporation at high vacuum. Unless otherwise specified, the effective device area is 0.045 cm^2. In addition to the fabrication process of ZnO CIL, all other fabrication processes were carried out in a N_2-filled glovebox.

For the fabrication of rigid devices, the PFOPy and PFOPy-N CILs were thermally crosslinked by optimized annealing of 180 ℃ for 10 min and 140 ℃ for 10 min, respectively. For the fabrication of flexible devices, PFOPy, PFOPy-N and ZnO CILs were separately deposited on PET/ITO substrate and mildly annealed at 100 ℃ for 10 min due to the poor temperature tolerance of PET substrate.

Thickness evaluation of ultrathin cathode interlayer (CIL)

PFOPy or PFOPy-N CILs with different thickness were prepared by changing the concentration of PFOPy or PFOPy-N solution, and absorption spectra of PFOPy or PFOPy-N CILs with different thickness were measured by UV-vis spectrophotometry. Then, the linear relationship of absorption intensity (at 358 nm) with the film thickness was established to determine the film thickness of PFOPy or PFOPy-N CILs, where relatively large thickness of CILs is measured by Bruker step profile.

Measurements and characterization

The current density–voltage (*J-V*) characteristics of OSCs were measured by using a computer-controlled Keithley 2450 source meter measurement system (Enlitech) with an AM 1.5G filter at an illumination intensity of 100 mW cm^{-2}, and the power of the sun simulation was calibrated before the testing by using a standard silicon solar cell.

The external quantum efficiency (EQE) of OSCs was measured in air by using a commercial measurement system (Enlitech). For the thermal cycling stability measurement of OSCs, the devices were simply encapsulated by a cover slide and subjected to the identical thermal cycling stress conditions, where a complete thermal cycle in ambient atmosphere consisted of four stages: (1) the devices were stored at ~2 °C for 5 h in a refrigerator; (2) the devices were placed in air at room temperature (RT) for 2 h; (3) the devices were baked at ~60 °C for 5 h in an oven; (4) the devices were restored to RT by repeating step 2 and then measured to obtain photovoltaic parameters.

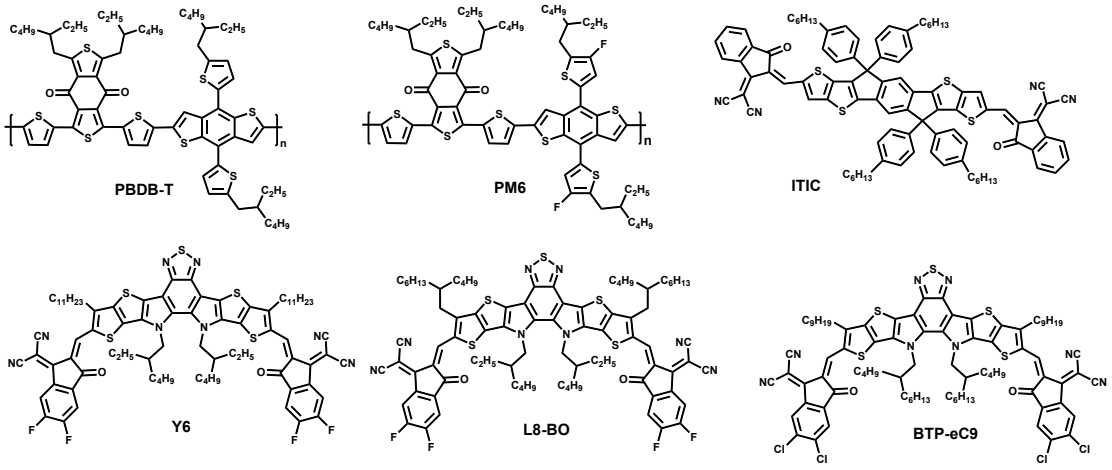

Figure S1. Chemical structures of PBDB-T, PM6, ITIC, Y6, L8-BO, and BTP-eC9.

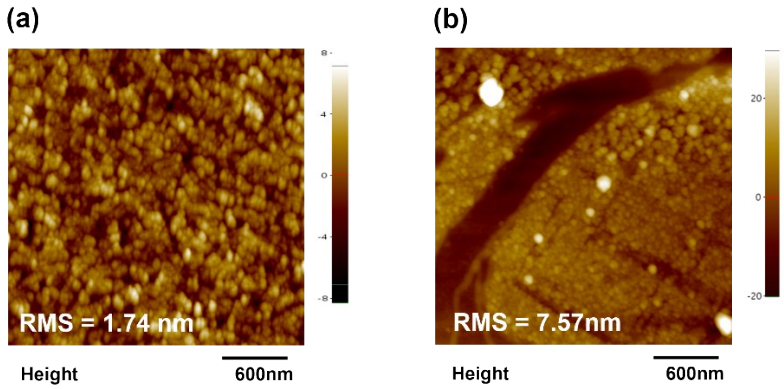

Figure S2. Surface AFM height images of PDINN cathode interlayers (a) before and (b) after washing with chloroform (CF).

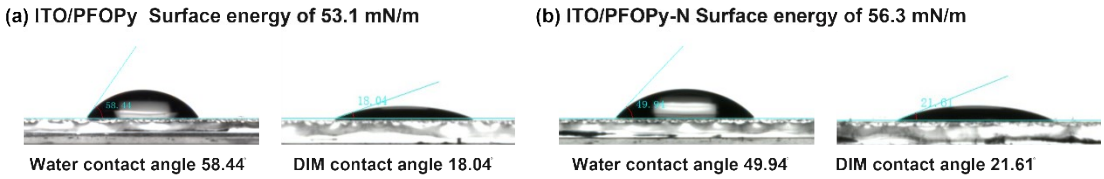

Figure S3. Surface energy of the PFOPy and PFOPy-N CILs were analyzed by measuring surface contact angle with water and diiodomethane (DIM).

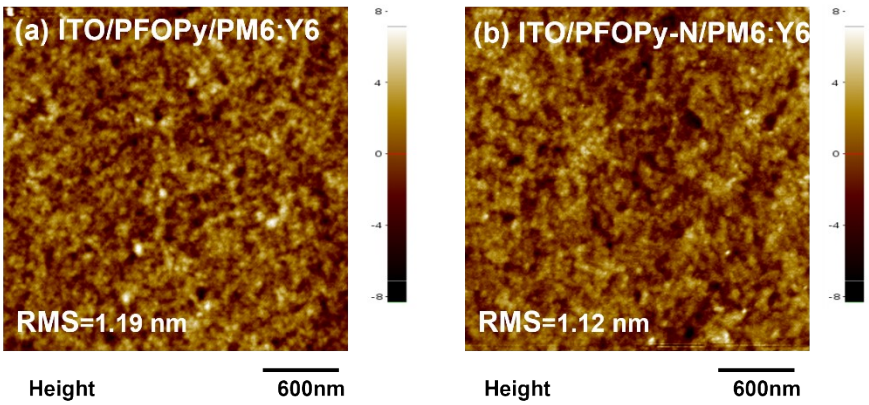

Figure S4. Surface AFM height images of PMY:Y6 active layers on (a) PFOPy and (b) PFOPy-N cathode interlayers.

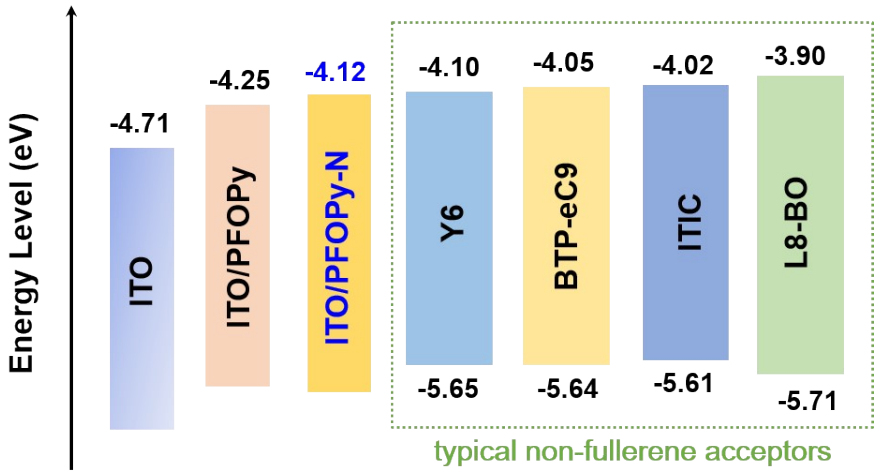

Figure S5. Energy levels diagram of ITO with different CILs and typical non-fullerene acceptors.

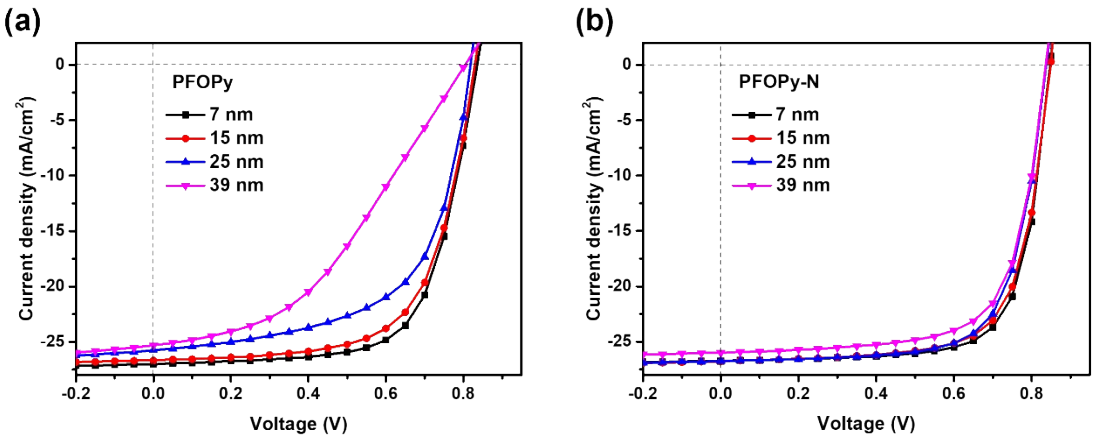

Figure S6. *J-V* curves of inverted OSCs based on (a) PFOPy and (b) PFOPy-N CILs with different thickness.

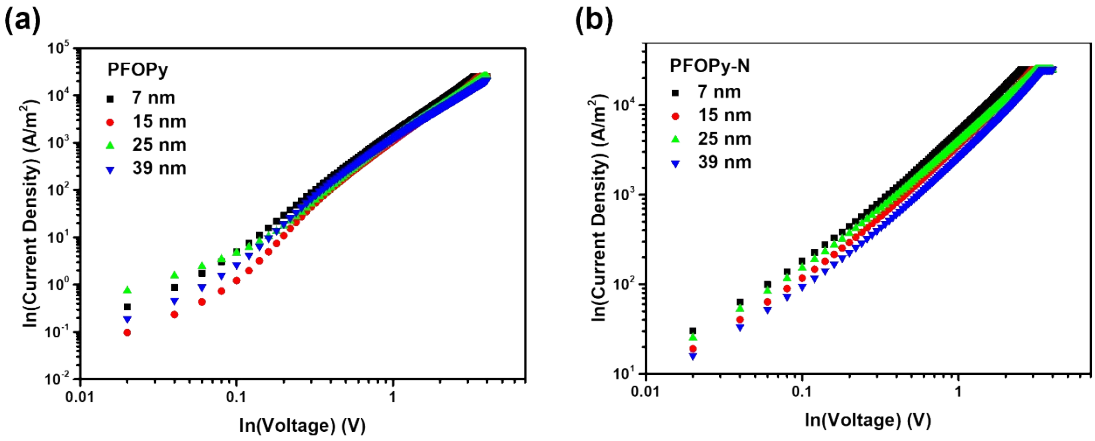

Figure S7. *J-V* curves of electron-only devices based on (a) PFOPy and (b) PFOPy-N CILs with different thickness.

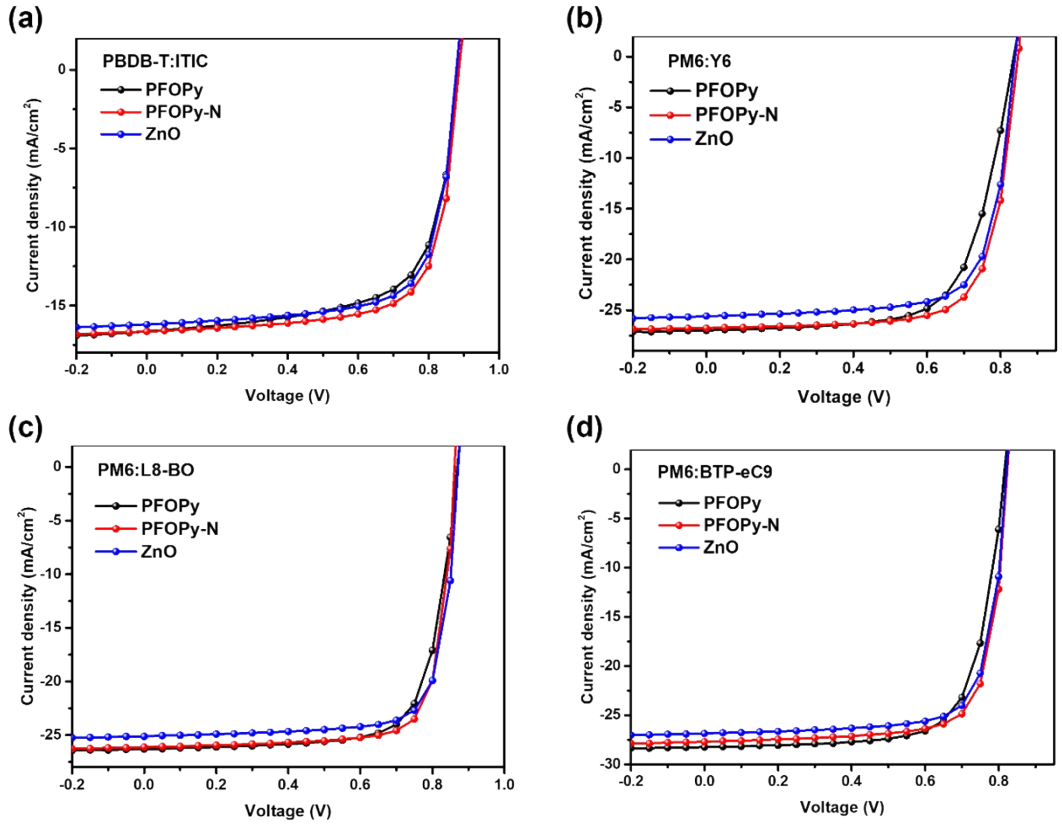

Figure S8. *J-V* curves of inverted OSCs with different cathode interlayers for different non-fullerene active layers: (a) PBDB-T:ITIC, (b) PM6:Y6, (c) PM6:L8-BO and (d) PM6:BTP-eC9.

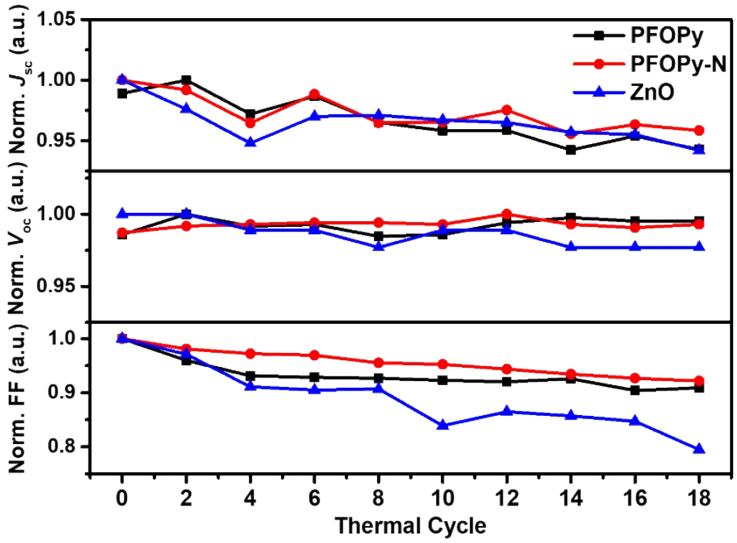

Figure S9. Normalized photovoltaic parameters of inverted OSCs with different cathode interlayers subjected to multiple thermal cycles.

Table S1. Photovoltaic parameters of inverted OSCs based on PFOPy-N CIL (7 wt% PDINN) with different annealing temperature for 10 min, under the illumination of AM 1.5 G, 100 mW/cm^2.

Temperature (°C)	V_{oc} (V)	J_{sc} (mA/cm^2)	FF (%)	PCE (%)
100	0.840	26.07	68.86	15.08
140	0.840	26.82	70.39	15.87
180	0.838	26.81	69.49	15.62

Table S2. Photovoltaic parameters of inverted OSCs based on PFOPy-N CIL with different PDINN contents, under the illumination of AM 1.5 G, 100 mW/cm^2.

wt% of PDINN	V_{oc} (V)	J_{sc} (mA/cm^2)	FF (%)	PCE (%)
7	0.840	26.50	71.00	15.80
10	0.847	26.77	73.19	16.60
14	0.837	27.05	73.13	16.56
20	0.836	26.83	71.77	16.10
40	0.831	26.49	67.48	14.85
100	0.821	24.90	61.64	12.61

Table S3. The device resistance fitting results of inverted OSCs with PFOPy and PFOPy-N CILs by impedance spectroscopy measurement.

CIL	R_S (Ω)	R_{CT} (Ω)	C1 (F)
PFOPy	7.92	1131	1.082×10^{-9}
PFOPy-N	4.21	211	9.190×10^{-10}

Table S4. Photovoltaic parameters of inverted OSCs based on PFOPy and PFOPy-N CILs with different thickness, under the illumination of AM 1.5 G, 100 mW/cm^2.

CIL	thickness (nm)	V_{oc} (V)	J_{sc} (mA/cm^2)	FF (%)	PCE (%)
PFOPy	7	0.836	27.02	67.72	15.29
	15	0.829	26.67	65.61	14.51
	25	0.818	25.75	60.51	12.75
	39	0.804	25.31	41.28	8.39
PFOPy-N	7	0.847	26.77	73.19	16.60
	15	0.849	26.80	70.99	16.15
	25	0.837	26.76	70.41	15.78
	39	0.836	26.02	69.22	15.06

Table S5. The calculated μ_e values of electron-only devices based on PFOPy and PFOPy-N CILs with different thickness.

CIL	thickness (nm)	Active Layer Thickness (nm)	μ_e (cm^2/V/S)
PFOPy	7	100	7.36×10^{-4}
	15	100	5.79×10^{-4}
	25	100	5.66×10^{-4}
	39	100	4.66×10^{-4}
PFOPy-N	7	100	1.08×10^{-3}
	15	100	7.91×10^{-4}
	25	100	7.15×10^{-4}
	39	100	5.77×10^{-4}

Table S6. Photovoltaic parameters of inverted OSCs with different CILs for different

active layers of PBDB-T:ITIC, PM6:Y6, PM6:L8-BO and PM6:BTP-eC9, under the illumination of AM 1.5 G, 100 mW/cm^2.

Active layer	CIL	V_{oc} (V)	J_{sc} (mA/cm^2)	FF (%)	PCE (%)
PBDB-T:ITIC	PFOPy	0.885	16.64	66.54	9.80
	PFOPy-N	0.886	16.65	71.86	10.60
	ZnO	0.880	16.07	71.57	10.21
PM6:Y6	PFOPy	0.836	27.02	67.72	15.30
	PFOPy-N	0.847	26.77	73.19	16.60
	ZnO	0.839	25.57	73.41	15.75
PM6:L8-B0	PFOPy	0.861	26.37	73.53	16.69
	PFOPy-N	0.862	26.12	78.37	17.65
	ZnO	0.871	25.13	77.70	17.01
PM6:BTP-eC9	PFOPy	0.816	28.24	72.01	16.60
	PFOPy-N	0.823	27.72	76.28	17.41
	ZnO	0.821	26.86	76.25	16.81

Table S7. The photovoltaic parameters statistics of inverted OSCs with different organic cathode interlayers.

CIL	Type	Active Layer	V_{oc} (V)	J_{sc} (mA·cm^{-2})	FF (%)	PCE (%)	Area (cm^2)	Ref.
c-NDI:PCy$_2$	Rigid	PBDB-TF:BTP-eC9	0.83	28.30	75.40	17.70	0.039	5
c-NDI:PCy$_2$	Rigid	PBDB-TF:BTP-eC9	0.83	28.10	65.60	15.40	1.0	5
c-NDI:PCy$_2$	Rigid	PBDB-TF:Y6	0.84	27.50	73.10	16.90	0.039	5
NDI-B	Rigid	PBDB-TF:BTP-eC9	0.84	26.68	77.00	17.23	0.04	6
NDI-B	Rigid	PBDB-TF:BTP-eC9	0.84	25.83	74.57	16.18	1.0	6
N-TBHOB	Rigid	PM6:Y6	0.84	26.33	75.64	16.78	0.04	7
PFOPy-N	Rigid	PM6:Y6	0.85	26.77	73.19	16.60	0.045	This Work
PFOPy-N	Rigid	PM6:BTP-eC9	0.82	27.73	76.28	17.41	0.045	This Work
PFOPy-N	Rigid	PM6:L8-BO	0.86	26.12	78.37	17.63	0.045	This Work
PFOPy-N	Rigid	PM6:L8-BO	0.87	25.21	72.92	15.94	0.45	This Work
PFOPy-N	Flexible	PM6:L8-BO	0.86	25.38	72.59	15.84	0.045	This Work

Table S8. Photovoltaic parameters of large-area inverted OSCs with different CILs and PM6:L8-BO active layer, under the illumination of AM 1.5 G, 100 mW/cm^2.

device area	CIL	V_{oc} (V)	J_{sc} (mA/cm^2)	FF (%)	PCE (%)
0.45 cm^2	PFOPy	0.866	25.26	61.18	13.38
0.45 cm^2	PFOPy-N	0.867	25.21	72.96	15.95
0.45 cm^2	ZnO	0.874	24.90	72.61	15.80

Table S9. Photovoltaic parameters of flexible inverted OSCs with different CILs and PM6:L8-BO active layer, under the illumination of AM 1.5 G, 100 mW/cm^2.

CIL	annealing temp.	V_{oc} (V)	J_{sc} (mA/cm^2)	FF (%)	PCE (%)
PFOPy	100 ℃ 10 min	0.812	25.55	54.92	11.40
PFOPy-N	100 ℃ 10 min	0.859	25.38	72.59	15.84
ZnO	100 ℃ 10 min	0.838	1.54	20.14	0.01

[1] P. Cai, X. Huang, T. Zhan, G. Chen, R. Qiu, L. Zhang, X. Xue, Z. Wang, J. Chen, ACS Appl. Mater. Interfaces 2021, 13, 12296-12304.

[2] C. Song, X. Huang, T. Zhan, L. Ding, Y. Li, X. Xue, X. Lin, H. Peng, P. Cai, C. Duan, J. Chen, ACS Appl. Mater. Interfaces 2022, 14, 40851-40861.

[3] Y. Cui, H. Yao, J. Zhang, K. Xian, T. Zhang, L. Hong, Y. Wang, Y. Xu, K. Ma, C. An, C. He, Z. Wei, F. Gao, J. Hou, Adv. Mater. 2020, 32, 1908205.

[4] P. Cai, P. Ren, X. Huang, X. Zhang, T. Zhan, J. Xiong, X. Xue, Z. Wang, J. Zhang, J. Chen, Adv. Mater. Interfaces 2020, 7, 1901912.

[5] Y. Yang, J. Wang, Y. Zu, Q. Liao, S. Zhang, Z. Zheng, B. Xu, and J. Hou, Joule 2023, 7, 545-557.

[6] Q. Liao, Q. Kang, Y. Yang, Z. Zheng, J. Qin, B. Xu, J. Hou, CCS Chem. 2022, 4, 938–948.

[7] L. Wang, Y. Chen, W. Tao, K. Wang, Z. Peng, X. Zheng, C. Xiang, J. Zhang, M. Huang, B. Zhao, Macromol. Rapid Commun. 2022, 2200119.